UCRL-92802
PREPRINT

SUBTHRESHOLD PION PRODUCTION

Marshall Blann
University of California
Lawrence Livermore National Laboratory
Livermore, CA 94550

This paper was prepared for submittal to
Physical Review C

June 1985

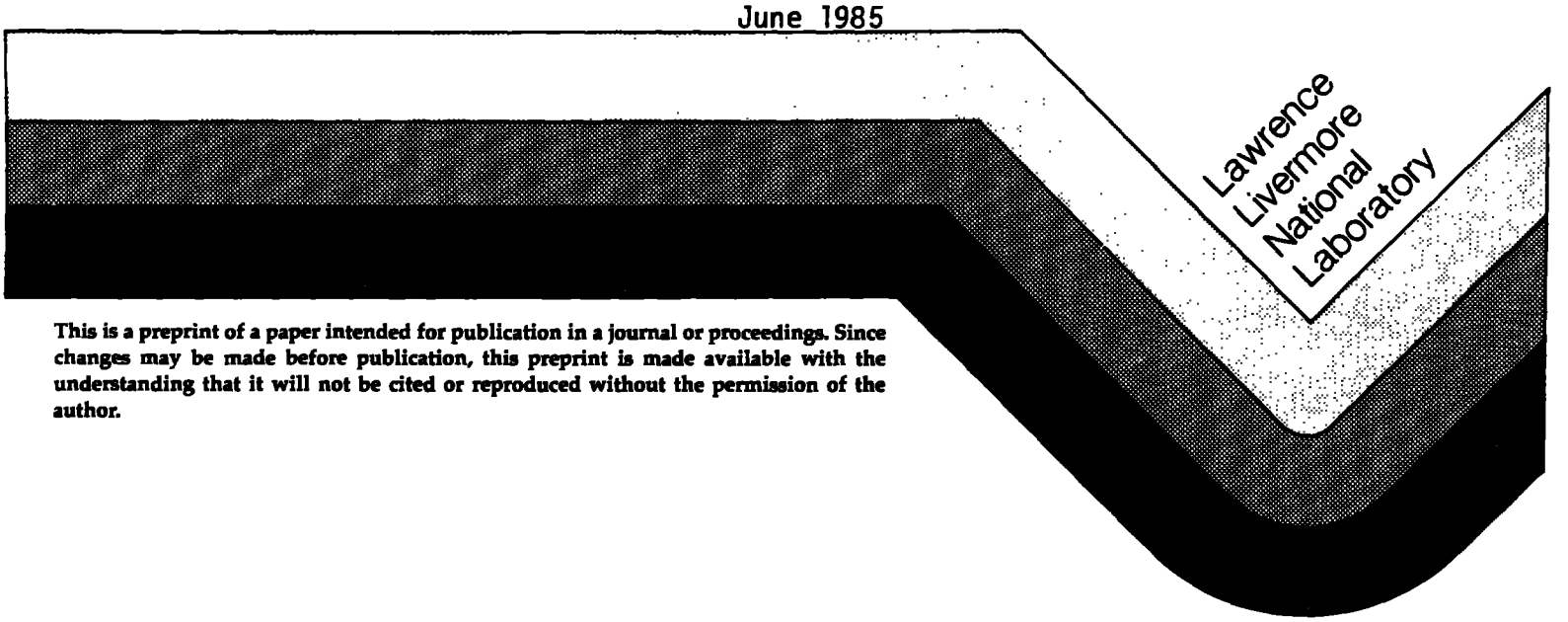

SUBTHRESHOLD PION PRODUCTION

M. Blann
Lawrence Livermore National Laboratory
University of California
Livermore, CA 94550

ABSTRACT

The Boltzmann master equation as adopted for treating equilibration in heavy ion reactions has been modified to include pion production rates from (n,n), (n,p) and (p,p) collisions. We calculate neutral pion production cross sections for reactions of 35 MeV/nucleon ^{14}N with ^{27}Al, ^{58}Ni and ^{184}W targets. We also calculate π° production cross sections for reactions of $^{12}C + ^{12}C$, ^{58}Ni, ^{238}U at beam energies of 60, 74 and 84 MeV/nucleon, and of 44 MeV/nucleon ^{40}Ar with ^{40}Cu, ^{119}Sn and ^{238}U. Results of these calculations are generally within a factor of 2 of experimental values. Compound nucleus excitations predicted for the equilibrated nuclei for the above reactions are also estimated for implications in a compound nucleus interpretation of the pion production mechanism.

I. INTRODUCTION

A great deal of work has been done regarding experimental measurement and theoretical interpretation of 'subthreshold' pion production.[1-12] This involves reactions of heavy ions with beam velocities below the energy per nucleon required to produce pions in free nucleon-nucleon collisions, yet with the collective energy of the projectile bringing energy in excess of the pion mass to the composite system. The question is how the collective energy shared by many of the projectile nucleons becomes available for pion production.

One suggestion is that the coupling of the projectile beam velocity with the Fermi momenta of the nucleons gives enough energy to a few nucleons that they may undergo intranuclear collisions with sufficient energy to produce pions.[13] In the present work we will investigate the question as to whether or not such a mechanism is semi-quantitatively in agreement with existing experimental data. This will give an answer to the question 'might such a mechanism be responsible for the experimental results given reasonable input to the calculations? It can not, of course, prove that this is the correct mechanism. We will investigate the question by following the relaxation process of the composite system via the Boltzmann master equation model (BME) originally encoded by Harp, Miller and Berne.[14,15] We will also investigate the energy which this model predicts is removed during the equilibration process, as this is germane to model interpretations involving pion production from a compound nucleus (fully equilibrated) system.[4,5]

In Section II the master equation and input will be defined and discussed. In Section III we compare results of this equation with experimental measurements of π° produced from 35 MeV/nucleon ^{14}N on

several targets, and from $^{12}C + {}^{12}C$, ^{58}Ni and ^{238}U reactions at energies of 60 to 84 MeV/nucleon and $^{40}Ar + {}^{40}Ca$, ^{119}Sn and ^{238}U at 44 MeV/nucleon. We will illustrate the dependence of results on input parameters, and suggest those experimental measurements which would help in reducing the uncertainties in the range of input variables. Conclusions will be presented in Section IV.

II. BOLTZMANN MASTER EQUATION AND INPUT FOR PION PRODUCTION CALCULATION

The Boltzmann master equation as written by Harp, Miller and Berne[14,15] considers the nucleus to be a two component Fermi gas, with all transitions taking place by two-body collisional processes. The master equation describing the proton collisional relaxation and emission is represented by

$$\begin{aligned}
\frac{dn_i^P}{dt} = & \sum_{jkl} \left[\omega_{kl\to ij}^{PP}\, g_k^P g_l^P n_k^P n_l^P (1 - n_i^P)\,(1 - n_j^P)\right] \\
& - \left[\omega_{ij\to kl}^{PP}\, g_g^P g_k^P g_l^P n_i^P n_j^P (1 - n_k^P)\,(1 - n_l^P)\right] \delta(\epsilon_i^P + \epsilon_j^P - \epsilon_l^P - \epsilon_k^P) \\
& + \sum_{jkl} \left[\omega_{kl\to ij}^{PN}\, g_k^P g_l^N g_j^N n_l^N n_k^P (1 - n_i^P)\,(1 - n_j^N)\right. \\
& \left. - \omega_{ij\to kl}^{PN}\, g_j^N g_l^N g_k^P n_i^P n_j^N (1 - n_k^P)\,(1 - n_l^N)\right] \delta(\epsilon_l^P + \epsilon_j^N - \epsilon_k^P - \epsilon_l^P) \\
& - n_{i'}^P \omega_{i'\to i}^P g_{i'}^P\, \delta(\epsilon_{i'}^P - \epsilon_i^P + \epsilon_f^P + B_p) \quad ,
\end{aligned} \tag{1}$$

$$i = 1, \ldots \epsilon_f^P + E^* \quad ,$$
$$i' = 1, \ldots E^* - {}_pB$$

where the symbols used are defined in Table I. A similar set of equations defines the relaxation and particle emission of the neutron gas.

The transition probabilities are defined classically

$$\omega^{pp}_{ij\to kl} = \frac{\sigma_{pp}(\epsilon^p_i + \epsilon^p_j)[(2/M)(\epsilon^p_i + \epsilon^p_j)]^{1/2}}{V\sum'_{mn} g^p_m g^p_n \sigma(\epsilon^p_i + \epsilon^p_j - \epsilon^p_m - \epsilon^p_n)} \quad , \tag{2}$$

with symbols defined in Table I. All nucleon-nucleon scattering cross sections are given by the equations due to Chen et al.[16] for free nucleon-nucleon scattering based on total nucleon energy i + j corresponding to an average collision angle of 90°. The master equation follows the rate at which nucleons in each energy bin can scatter with all other nucleons, or be emitted into the continuum, in time intervals short (2×10^{-23} sec) with respect to the average N-N collision period.

The HMB code has been modified to include a channel in which three body final states may exist[12]; in particular

$$n + n \to n + n + \pi^\circ \tag{3a}$$

$$p + p \to p + p + \pi^\circ \tag{3b}$$

$$p + n \to p + n + \pi^\circ \tag{3c}$$

$$p + n \to d + \pi^\circ \quad . \tag{3d}$$

The energy dependent cross sections (3b-d) which we use are from the work of Ver West and Arndt[17]; we assume that (3a) and (3b) have identical cross sections. We add the cross sections (3c) and (3d) for π° production rates in p-n collisions. We calculate rates for these pion producing reactions by

$$\omega^{pp\pi^\circ}_{ij\to k'l'm} = \frac{\sigma_{pp\pi^\circ}(\epsilon_i + \epsilon_j)[(2/M)(\epsilon^p_i + \epsilon^p_j)]^{1/2}}{V\sum'_{nop} g_n g_o g_p \delta(\epsilon^p_i + \epsilon^p_j - \epsilon^p_n - \epsilon^p_o - \epsilon^\pi_p - m_{\pi^\circ})} \quad , \tag{4}$$

with symbols defined in Table I, and with an analogous expression using $\sigma^{PN\pi^\circ}$ for neutron-proton collision processes.

The master equation (1) is then modified by a pion production term

$$\frac{dN^\pi}{dt} = \sum_{ijk'l'm} \omega_{ij\to k'l'm}^{PP\pi^\circ} g_m g_i^P g_j^P n_i^P n_j^P (1-n_{k'}^P)(1-n_{l'}^P) \qquad (5)$$

$$+ \sum_{ijk'l'm} \omega_{ij}^{PN\pi^\circ} g_m g_i^P g_j^N n_i^P n_j^N (1-n_{k'}^P)(1-n_{l'}^N)$$

$$+ \sum_{ijk'l'm} \omega_{ij}^{NN\pi^\circ} g_m g_i^N g_j^N n_i^N n_j^N (1-n_{k'}^N)(1-n_{l'}^N) \quad ,$$

with symbols defined in Table I. The sums are over all energy pairs i+j such that $k'+l'+m+m_\pi = i+j$. Implicit in this approach is the assumption that we may reasonably treat the final state as three body in nature near threshold, rather than as being dominated by a Δ final state. If this is not a good assumption, we feel that the shape of the final π° spectrum would be affected more adversely than the total production rate which depends primarily on the $\sigma^{PP\pi^\circ}$, $\sigma^{PN\pi^\circ}$, and $\sigma^{NN\pi^\circ}$ values versus incident nucleon energies. The threshold energy, i+j, for pion production is 280 MeV in our calculation.

The HMB model code was modified to use a time dependent injection of nucleons into a nuclear system, as might be encountered in a heavy ion reaction where nucleons from a projectile interact with target nucleons after passing through a neck region.[18,19] For simplicity we assume a projectile approach at constant velocity given by the projectile energy decreased by the coulomb barrier height. Results are not sensitive to the details of the assumed time dependence of the coalescence process, but they are very sensitive to the assumed energy dependence of the coalescing nucleon excitations.

For the latter we have made several assumptions. Results of calculations for pion production rates will be considerably more sensitive to the quantitative merit of these assumptions than will nucleon emission spectra. We will try to illustrate this point in the results to be presented. This exercise will point out the types of experimental measurements which might better restrict the range of input parameters for the pion production calculation.

Our assumptions for the initial exciton distribution function involve the following: the projectile nucleons have a beam velocity with which they approach the target. Additionally there is a velocity distribution of nucleons within the projectile due to the Fermi momenta. We assume that the projectile nucleons entering the target may therefore have energies from the target Fermi energy, to the target Fermi energy plus the maximum energy resulting from the coupling of the projectile Fermi and beam velocities, or the maximum excitation energy available to the composite nucleus, whichever is less. The distribution function used is based on the assumption that some number of excitons share the total available excitation energy with every allowed energy partition equally likely. The distribution function is discussed in greater detail in Ref. 20, where we calculated precompound neutron spectra from the bombardment of ^{165}Ho with 220, 292 and 402 MeV ^{20}Ne ions.[21] In that work we found that a distribution function given by an exciton number equal to the projectile mass number to perhaps 3 greater than the projectile mass number gave a reasonable prediction of both the shape and absolute magnitude of the experimentally measured neutron spectra up to the 70 MeV experimental neutron energy limit. We show this result in Fig. 1.

The agreement of Fig. 1 supports the assumed exciton distribution function as being in agreement with nature up to 70 MeV neutron energy, and

probably somewhat beyond. However pion production requires collision of nucleons with 140 MeV or more above the bottom of the Fermi sea. We do not have evidence such as that of Fig. 1 to support our distribution function for the very tail of the exciton distribution function which is relevant to pion production. Measurements of the type shown in Fig. 1 to much higher neutron energies would provide the information necessary to an independently supported exciton distribution function to be used for pion production calculations. Such measurements are difficult because coincidence measurements are required, with the very small cross sections becoming ever smaller with increasing neutron energy. The evaporation residue like fragment would require detection with a large solid angle device (e.g. a recoil spectrometer) for such a coincidence measurement

The sensitivity of results of these calculations may be illustrated by comparing the distribution function versus energy for three cases. This is done in Fig. 2, where we show the distribution function for a ^{14}N projectile at 35 MeV/nucleon assuming 35 MeV projectile Fermi energy with 14 excitons, 40 MeV projectile Fermi energy with 14 excitons, and 35 MeV Fermi energy with 17 excitons. The pion production rate (14 excitons) increases by 60% between the distribution functions assuming 35 and 40 MeV projectile Fermi energy, due entirely to the small tail extending to higher energies in the latter case. The neutron spectra up to 70 MeV, on the contrary, are identical for either distribution function! Similarly in going from 14 to 17 excitons, the neutron spectra at 70 MeV will decrease by 40%, while the pion production rate will decrease by 70%. We see that there is a reasonably large uncertainty in results from calculations of the type we perform due to uncertainties in the input. Independent experiments (high energy nucleon emission spectra) may ultimately allow us to narrow the range of 'acceptable' input. At present we

proceed to use what seem to be reasonable values, bearing in mind the uncertainties in final results arising due to our ignorance in the input. For results to be presented (e.g. table II) we assume a target radius parameter of R_o = 1.2 fm (Fermi energy 30 MeV), and projectile Fermi energy of 35 MeV.

There is an additional point which must be emphasized as a possible weak point in the pion production calculation. The N-N collision cross sections are for average 90° collision angles; the Boltzmann equation as we use it follows energies, and not momenta. For pion production the high momentum components are most important, and these are more likely (initially) to be parallel rather than at 90°, when both partners are from the primal projectile source.

The calculation as described thus far provides a prediction of the number of pions produced per target-projectile interaction. Experimental measurements report the cross sections of emitted pions. These two points are connected by a bridge of additional assumptions. These primarily include the pion mean free path in nuclear matter, and the cross section for collisions which are sufficiently central to participate in the pion production process. Our approach to these questions is arbitrary and simple; the uncertainties already discussed do not justify very sophisticated answers.

The mean free path of a pion is thought to be reasonably independent of energy for pions above 20 MeV, with a mean free path of around 3 fm.[22] The average impact parameter for a reaction comes at around 0.7 of the maximum radius. We therefore have assumed pions produced at $0.7 \times 1.2 \times 10^{-13} (A_T + A_p)^{1/3}$ cm. We assume that half the pions move radially away from the nuclear center and half toward the center. We calculate an energy attenuation factor, assuming a 3 fm mean free path, based on this simple picture. The

values so calculated are summarized in Table II. For the reaction cross sections we have used

$$\sigma_R = \pi \cdot [1.2 \times 10^{-13}(A_T^{1/3} + A_p^{1/3})]^2 \quad . \tag{6}$$

Results of Eq. (6) for the target-projectile combinations considered herein are summarized in Table II.

III. RESULTS AND DISCUSSION

In Fig. 3 we show experimental π° production cross sections for 35 MeV/nucleon ^{14}N with targets of ^{27}Al, ^{58}Ni and ^{184}W, compared with calculated results as described in Section II. The calculated results in Fig. 3 result from assuming a Fermi energy of 35 MeV and a distribution function characterized by 14 excitons. These results, and those for the other systems considered, are summarized in Table II. Generally the calculated results agree to within a factor of two or better with experimental measurements for all cases considered, with the exception of $^{40}Ar + ^{40}Ca$ at 44 MeV/nucleon incident energy. For this example the calculated yields are low by a factor of 6. We see no obvious explanation for this discrepancy. The direction of discrepancies for the $^{12}C + ^{12}C$, ^{58}Ni yields with increasing projectile energy is consistent with a reaction cross section which decreases with increasing projectile energy, a reasonable expectation not contained in the simple Eq. (6) used. The agreement shown between calculated and experimental results in Table II suggests that the nucleon-nucleon collision mechanism may very well be one viable explanation of the yields of subthreshold pion production.

If this is the case, then the pion production provides a probe of the very early time history of a heavy ion reaction, as indicated in Fig. 4. The production rate of pions via the two body mechanism may be seen to go rapidly to zero after coalescence is complete, while the nucleon emission rate decreases much more slowly, finally asymptotically approaching an equilibrium emission rate of the order of 10% of the maximum pre-equilibrium rate. Pion production is therefore seen to be extremely sensitive to the primary exciton distribution, and quite insensitive to the distribution after even partial relaxation of the excited Fermi gas.

It has been suggested that subthreshold pion production results from the compound nucleus.[4,5] Such calculations should recognize that a great deal of excitation will be removed by nucleon emission prior to achieving equilibrium. In Table III we summarize predictions of the BME calculation described in this work, for the average compound nucleus excitation to be expected for several of the 'subthreshold' systems which have been investigated experimentally. The total excitations in several cases are far below the absolute pion production thresholds. All are at considerably lower excitations than the maximum excitation available to the composite systems. Stated differently, only an extremely small fraction of an ensemble of composite systems (for the cases summarized in Table III) might reasonably be expected to equilibrate prior to precompound decay. Pion production calculations for compound nuclei must find a reasonable method of calculating this fraction if the results are to be relevant to comparisons with experimental yields.

For interest we have summarized the most probable equilibrium quasi-particle numbers at maximum excitation energy for the systems considered herein. These are presented in the next to last column of Table II. The quasi-particle numbers actually used for the initial energy partitions in the BME are shown in the last column of Table II. All systems must evolve from an initial condition very far from equilibrium.

Pion spectra from the Boltzmann master equation are compared with experimental results in Fig. 5. The calculated results are seen to be too hard compared with experimental spectra. However the higher energy pions would be more likely to interact through the Δ resonance, and this would tend to soften the spectrum of observed pions. The disagreement in spectral shape is therefore qualitatively in the proper direction.

IV. CONCLUSIONS

The nucleon-nucleon collision mechanism which has been used to explain pion production in nucleon-nucleus collisions is a viable candidate to explain so called 'sub-threshold' pion production. The latter refers to reactions in which a heavy ion projectile has an energy per nucleon below the N-N-π production threshold, but total CM energy in excess of the threshold value.

Uncertainties in the input parameters of the calculation relating to the high energy tail of the energy distribution of coalescing nucleons introduce large uncertainties in the quantitative significance of the results of these calculations at this time. Experimental measurements of the nucleon emission spectra for central collisions and for nucleons in excess of $\approx$ 110 MeV should reduce the ambiguity in input for calculations of this type, thereby increasing confidence in the quantitative results of such calculations.

V. ACKNOWLEDGEMENTS

The author wishes to acknowledge helpful discussions with Profs. P. Braun-Munsinger and R. A. Arndt during the course of this work.

Work performed under the auspices of the U.S. Department of Energy by the Lawrence Livermore National Laboratory under contract number W-7405-ENG-48.

Table I. Definition of symbols.

Symbol	Definition
$n_i^X \omega_i^X \to i$	fraction of population of the nucleons of type X (neutron = N, proton = P) emitted per unit time from a bin at energy i measured from the bottom of the Fermi sea.
$\omega_{ij\to kl}^{XY}$	rate at which one nucleon of type X at energy i scatters with one nucleon of type Y at energy j into final energies k and l.
g_i^X	number of states for a particle of type X in a 1 MeV wide energy bin centered at energy i with respect to the Fermi energy.
n_i^X	fraction of the g_i^X levels in bin i which are occupied at time t.
B_X	binding energy of a nucleon of type X.
ϵ_i^X	single particle energy of a nucleon of type X in bin i, measured from the bottom of the Fermi sea.
$\omega_{i\to i'}^X$	rate at which a particle of type X at energy i with respect to the bottom of the nucleon well and energy i' with respect to the unbound continuum is emitted into the continuum.
$\delta(\epsilon_i^Y+\epsilon_j^P-\epsilon_k^P-\epsilon_l^P)$	unity when initial and final nucleon energies conserve energy, otherwise zero.
E*	composite system excitation energy.
V	the nuclear volume, calculated in this work using a square well with radius parameter 1.2 x 10^{-13}fm.
M	nucleon mass.
$\sigma^{XY}(\epsilon_i+\epsilon_j)$	cross section for a free nucleon of type X and energy ϵ_i to collide elastically with a free nucleon of type Y and energy ϵ_j.
$\sigma^{XY\pi^\circ}(\epsilon_i+\epsilon_j)$	cross section for a nucleon of type X at energy ϵ_i to collide with a nucleon of type Y at energy ϵ_j to produce a π° plus nucleons X and Y with final energies such that mass and energy are conserved.

Table II. Summary of calculated and experimental subthreshold pion production cross sections.

Projectile Target	MeV Nucleon	Calculated σ_R(a)	Calculated $f_{atten.}$(b)	Calculated Pions Interactions	Calculated Emitted Pions σ_{π^o} (μb)(c)	EXPTL σ_{π^o}(μb)	REF	E*(MeV)(g)	$\bar{n}$(h)	n_o(i)
$^{12}C/^{12}C$	60	0.96	0.42	0.41×10^{-5}	1.4	1.7(3)	d	374	31	12
	74			0.34×10^{-4}	14.	8.5(10)	d	458	34	12
	84			0.10×10^{-3}	40.	19.(23)	d	518	36	12
$^{12}C/^{58}Ni$	60	1.72	0.34	1.9×10^{-5}	11.	7.(1)	d	597	67	12
	74		0.34	1.26×10^{-4}	74.	31.(4)	d	736	74	12
	84		0.34	3.0×10^{-4}	175.	72.(9)	d	835	79	12
$^{12}C/^{238}U$	60	1.36	0.24	1.17×10^{-5}	9.2	13.(2)	d	661	133	12
	74		0.24	5.9×10^{-5}	46.	64.(10)	d	821	148	12
	84		0.24	1.4×10^{-4}	110.	174.(21)	d	936	158	12
$^{14}N/^{27}Al$	35	1.32	0.38	0.56×10^{-7}	0.028	0.070(10)	e	344	39	14
$^{14}N/^{58}Ni$	35	1.8	.34	0.1×10^{-7}	0.061	0.120(15)	e	395	55	14
$^{14}N/^{184}W$	35	3.0	.26	0.74×10^{7}	0.058	0.160(20)	e	440	97	14
$^{40}Ar/^{40}Ca$	44	2.1	0.33	4.7×10^{-7}	0.33	2.2(4)	f	880	87	40
$^{40}Ar/^{119}Sn$	44	3.14	0.27	3.1×10^{-6}	0.6	3.7(8)	f	1257	147	40
$^{40}Ar/^{238}U$	44	4.2	0.23	3.1×10^{-6}	2.9	6.(3)	f	1375	202	40

a) calculated as $(1.2(A_T^{1/3} + A_p^{1/3}) \times 10^{-13})^2 * \pi$ where A_T and A_p are target and projectile mass numbers.

b) attenuation factors, calculated as described in the text.

c) this is the product of the calculated reaction cross section times calculated pions per interaction times attenuation factor.

d) H. Noll et al., Phys. Rev. Lett. 48, 732 (1982).

e) J. Stachel et al., in Proceedings of the Institute for Nuclear Studies; RIKEN Symposium on Heavy Ion Physics, Tokyo, Japan, August 1984 (to be published).

f) H. Heckwolf et al., Z. Phys. A315, 243 (1984).

g) Composite nucleus excitation energy.

h) Equilibrium quasiparticle number for composite nucleus excitation.

i) Initial exciton number assumed in calculating pion production cross sections.

Table III. Average excitation energy at equilibrium calculated by Boltzmann equation for several systems.

Target	Projectile	E_{LAB}(MeV)	E_{CN}(MeV)[a]	E_{EQ}(MeV)[b]
^{184}W	^{14}N	490	440	197
^{58}Ni	^{14}N	490	395	190
^{27}Al	^{14}N	490	344	123
12C	^{12}C	720	374	85
^{12}C	^{12}C	888	458	99
^{12}C	^{12}C	1008	518	100

(a) Composite nucleus maximum excitation energy

(b) Calculated average excitation energy of equilibrated nuclei after precompound decay.

REFERENCES

1. P. Braun-Munzinger et al., Phys. Rev. Lett. 52, 255 (1984).
2. T. Johansson et al., Phys. Rev. Lett. 48, 732 (1982).
3. H. Noll et al., Phys. Rev. Lett. 52, 1284 (1984).
4. C. Gale and S. das Gupta, Phys. Rev. C 30, 4141 (1984).
5. J. Aichelin and G. Bertsch, Phys. Lett. 138B, 350 (1984).
6. J. Aichelin, Phys. Rev. Lett. 52, 2340 (1984).
7. D. Vask, H. Stoecker, B. Mueller, and W. Greiner, Phys. Lett. 93B, 243 (1980).
8. R. Shyam and J. Knoll, Gesellschaft für Schwerionenforschung Report No. GSI 83-22, 1983 (unpublished).
9. H. Heckwolf et al., Z. Phys. A315, 243 (1984).
10. J. Stachel et al., in Proceedings of the Institute for Nuclear Studies KIKEN Symposium on Heavy Ion Physics, Tokyo, Japan, August 1984 (to be published).
11. H. Kruse, B. V. Jacek and H. Stöcker, Phys. Rev. Lett. 54, 289 (1985).
12. M. Blann, Phys. Rev. Lett. 54, 2215 (1985).
13. G. F. Bertsch, Phys. Rev. C 15, 713 (1977).
14. G. D. Harp, J. M. Miller and B. J. Berne, Phys. Rev. 165, 1166 (1968).
15. G. D. Harp and J. M. Miller, Phys. Rev. C 3, 1847 (1971).
16. K. Chen et al., Phys. Rev. 166, 949 (1968).
17. B. J. Ver West and R. A. Arndt, Phys. Rev. C 25, 1979 (1982).
18. M. Blann, A. Mignerey, and W. Scobel, Nukleonika 21, 335 (1976).
19. M. Blann, Phys. Rev. 23, 205 (1981).
20. M. Blann, Phys. Rev. C 31, 1245 (1985).
21. E. Holub et al., Phys. Rev. C 28, 252 (1983).
22. P. Braun-Munzinger, private communication (1984).

FIGURE CAPTIONS

FIG. 1 Experimental and calculated precompound spectra for reactions induced by 220, 292, and 402 MeV (lab) ^{20}Ne ions on ^{165}Ho. The experimental points from Ref. 21 represent neutron spectra in coincidence with evaporation residues (open triangles) and fission fragments (closed circles). Calculated results are for initial exciton numbers of 20 (dashed curves) and 23 (line). A calculation using 20 excitons with the intranuclear transition rate divided by two is shown as a dotted curve for the 402 MeV case. All results are compared on an absolute, unnormalized basis.

FIG. 2 Exciton density distribution versus energy for projectile Fermi energies (ϵ_f) of 35 and 40 MeV, assuming initial exciton numbers of 14 and 17.

FIG. 3 Experimental and calculated π° yields for reactions of 35 MeV nucleon ^{14}N with ^{27}al, ^{58}Ni and ^{184}W targets. The experimental yields are from Ref. (1). The open squares are the calculated yields before multiplication by the attenuation factors noted in the text. The open circles are calculated results after multiplication by the attenuation factors summarized in Table II.

FIG. 4 Calculated π°, neutron emission and de-excitation rates versus time from the boltzmann master equation. The down arrow shows the time at which coalescence is considered to be complete in the BME. These results are for ^{184}W + 490 MeV ^{14}N. The rate of energy loss is on a relative scale on the ordinate. The abscissa gives pion or nucleon emission rates per time unit of 2×10^{-23} sec.

FIG. 5 Calculated and experimental π° spectra for 60 MeV/nucleon ^{12}C + ^{12}C, and for ^{84}MeV/nucleon ^{12}C + ^{238}U. Experimental results are from Ref. (3).

FIG. 6 Calculated and experimental π° spectra for 35 MeV/nucleon ^{14}N on ^{58}Ni. Experimental results are from Ref. (10).

1312v/43v

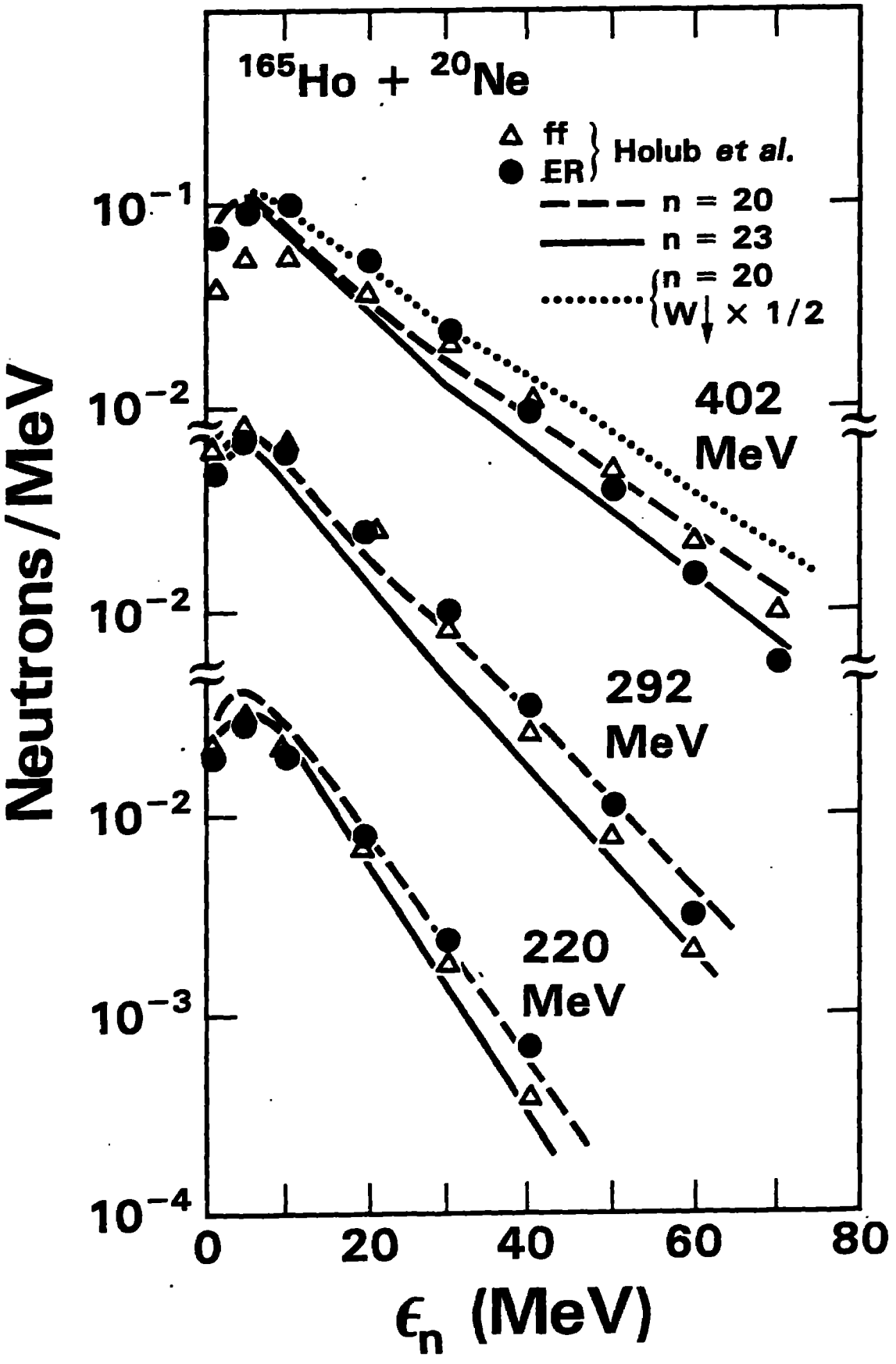
^{165}Ho + ^{20}Ne
ff
ER
Holub *et al.*
n = 20
n = 23
n = 20
W ↓ × 1/2
402 MeV
292 MeV
220 MeV
Neutrons / MeV
10^{-1}
10^{-2}
10^{-2}
10^{-2}
10^{-3}
10^{-4}
0
20
40
60
80
ϵ_n (MeV)

Fig. 1

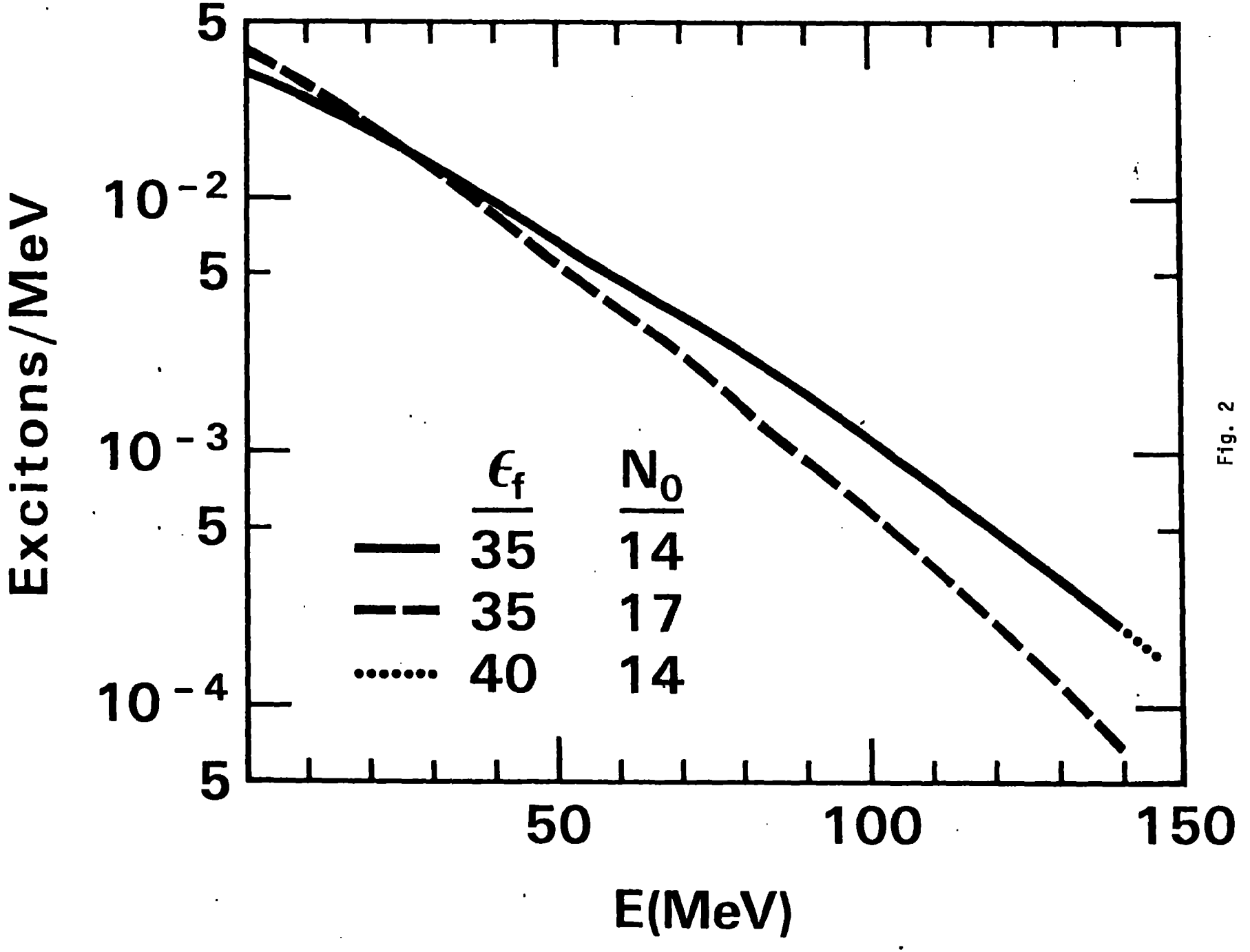
5
10^{-2}
5
10^{-3}
5
10^{-4}
5
Excitons/MeV
50
100
150
E(MeV)
ϵ_f N_0
35 14
35 17
40 14

Fig. 2

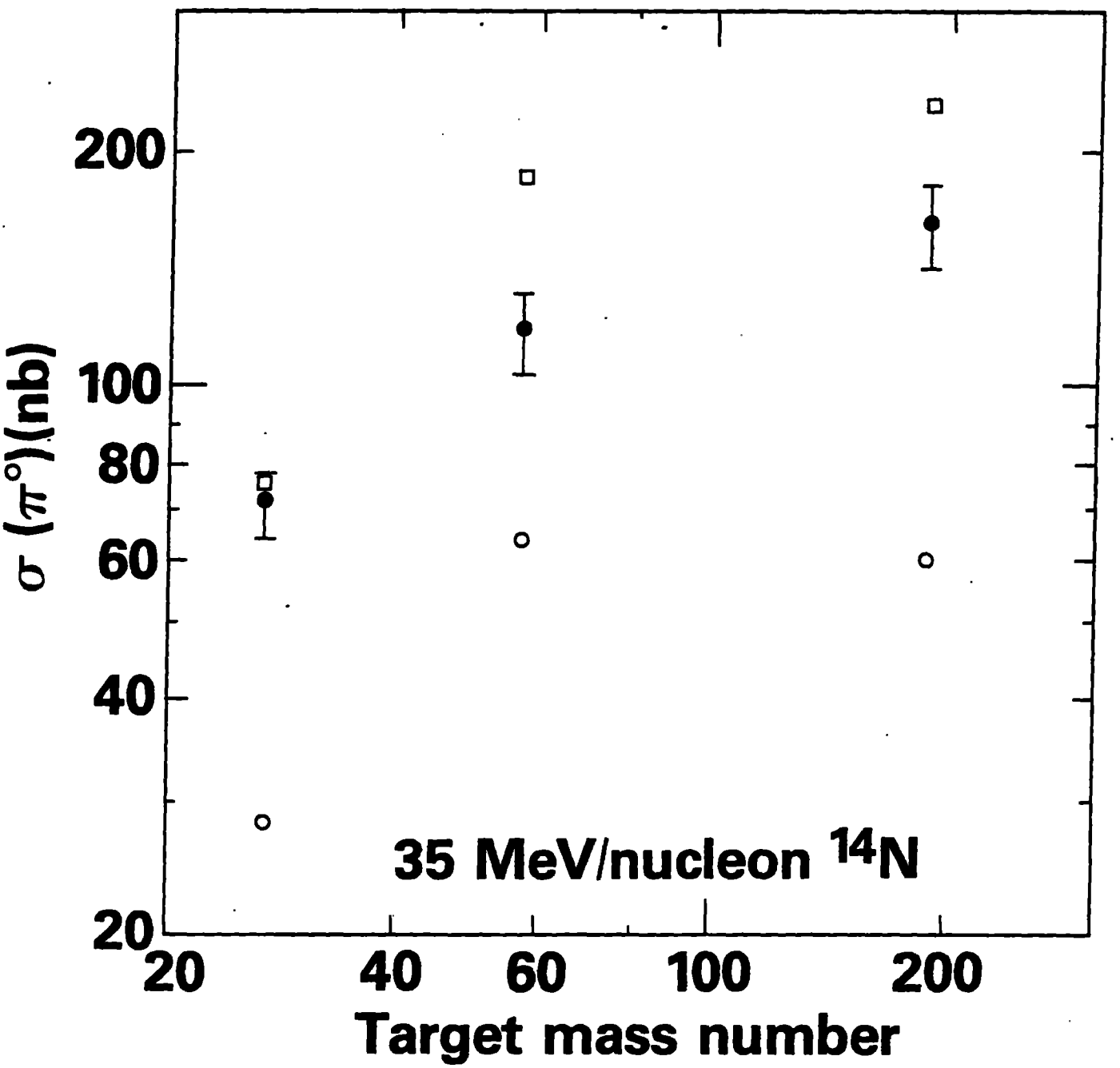
200
100
80
60
40
20
σ (π°)(nb)
35 MeV/nucleon 14N
20
40
60
100
200
Target mass number

Fig. 3

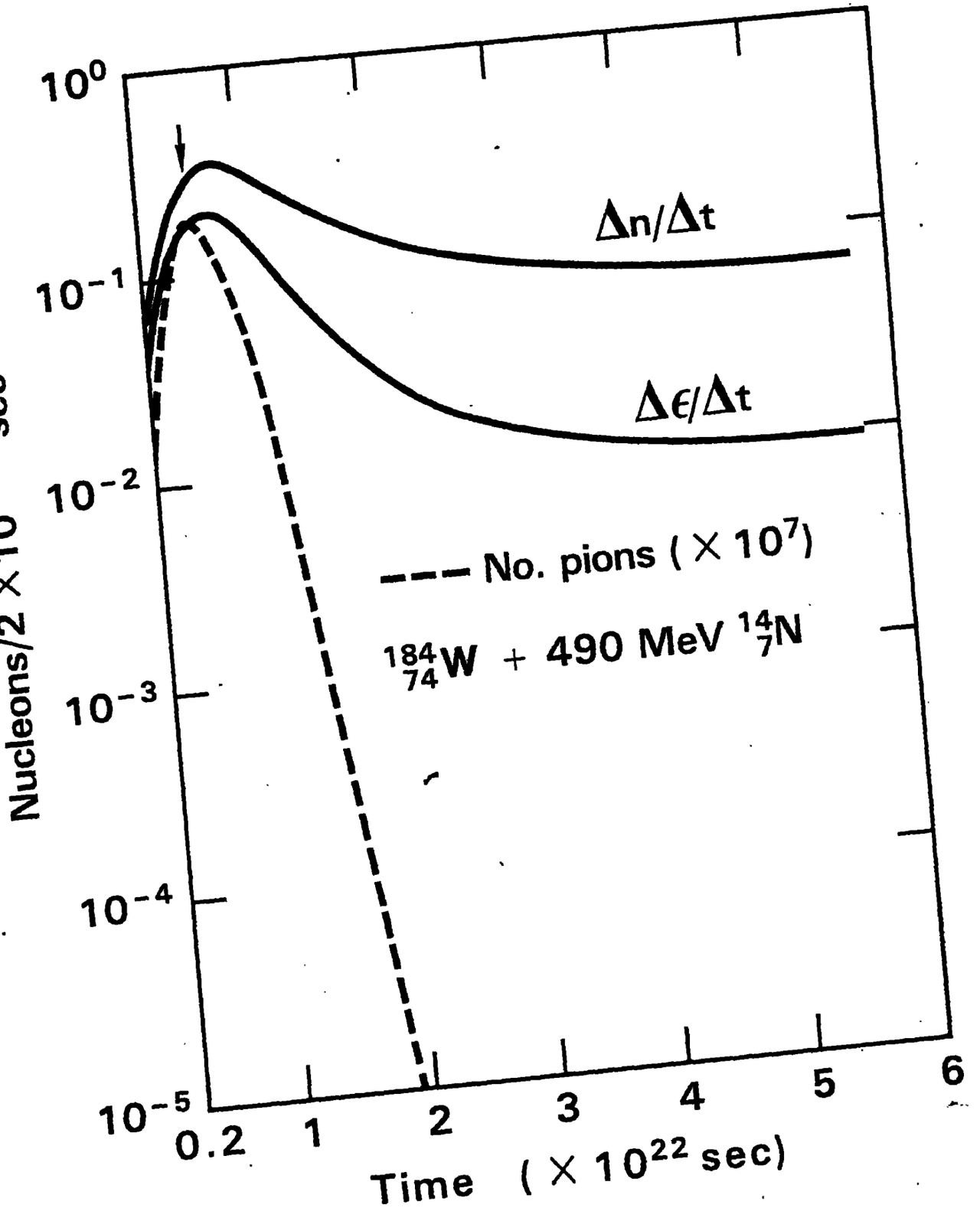
10^0
10^{-1}
10^{-2}
10^{-3}
10^{-4}
10^{-5}
Nucleons/2 $\times 10^{-23}$ sec
$\Delta n/\Delta t$
$\Delta \epsilon/\Delta t$
No. pions ($\times 10^7$)
$^{184}_{74}W$ + 490 MeV $^{14}_{7}N$
0.2
1
2
3
4
5
6
Time ($\times 10^{22}$ sec)

Fig. 4

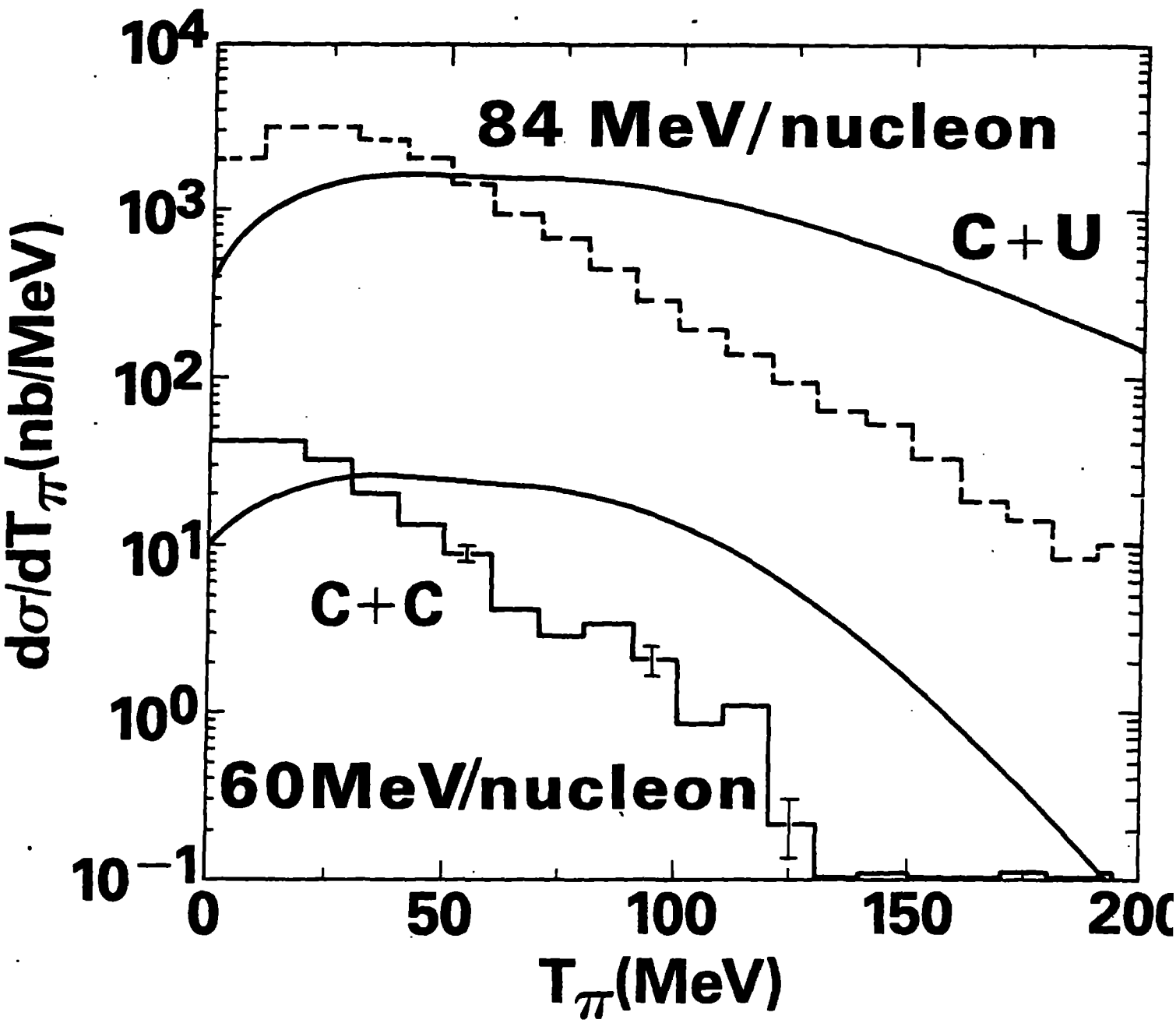
84 MeV/nucleon
C+U
C+C
60MeV/nucleon
$d\sigma/dT_\pi$(nb/MeV)
T_π(MeV)
10^4
10^3
10^2
10^1
10^0
10^{-1}
0
50
100
150
200

Fig. 5

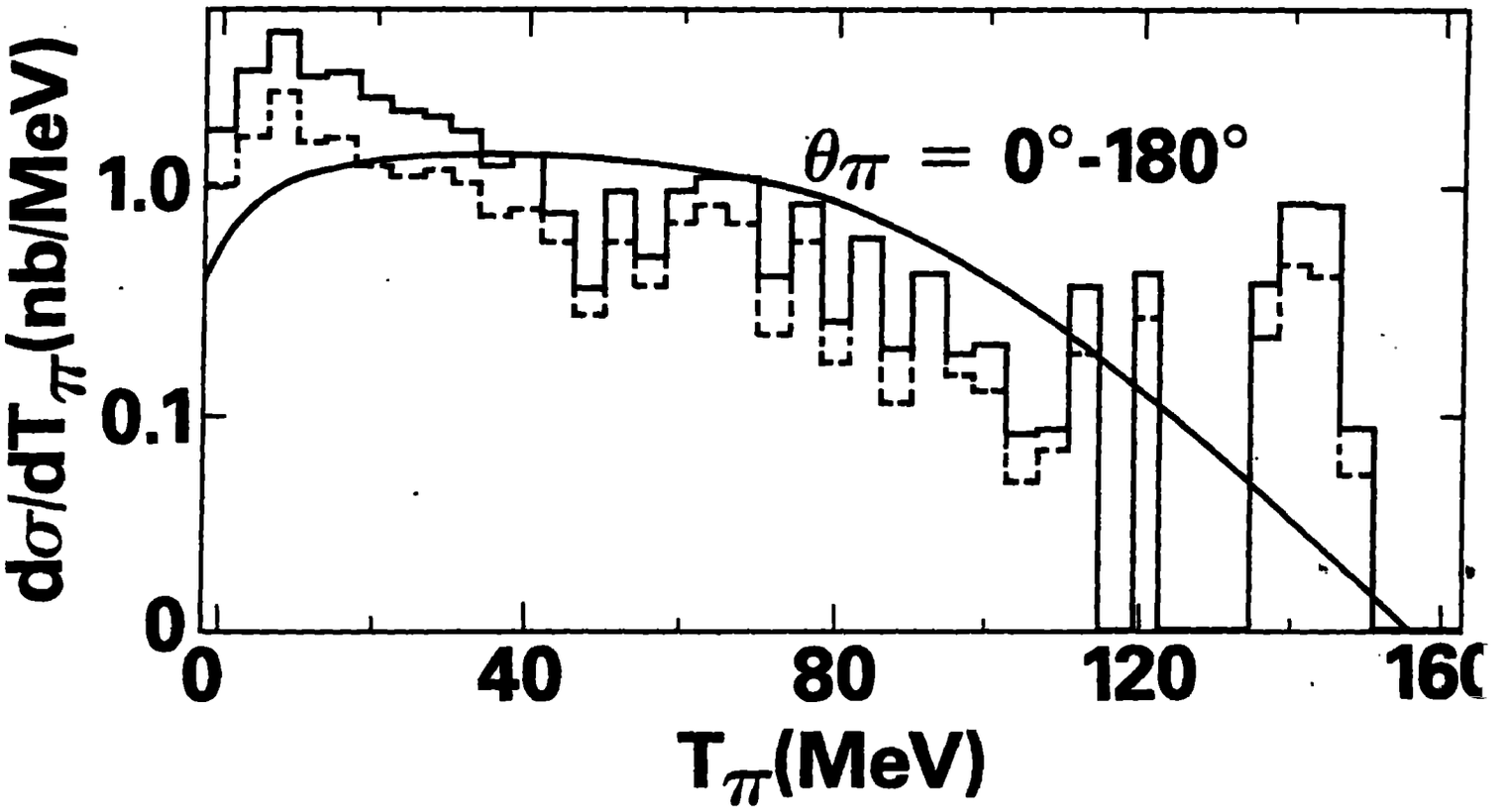

Fig. 6